The Morphology and Photoelectronic Properties of Poly(9,9′-dioctylfluorene)/Ethyl-Cyanoethyl Cellulose Blends

Benqiao He,[1,2] Jing Li,[2] Zhishan Bo,[2] Yong Huang[2]

[1]*Tianjin Key Laboratory of Fiber Modification and Functional Fiber, School of Materials and Chemical Engineering, Tianjin Polytechnic University, Tianjin 300160, China*
[2]*State Key Laboratory of Polymer Physics and Chemistry, Joint Laboratory of Polymer Science and Material, Beijing National Lab of Molecular Science, Institute of Chemistry, Chinese Academy of Sciences, Beijing 100080, China*

Received 4 December 2006; accepted 30 April 2007
DOI 10.1002/app.26768
Published online 12 July 2007 in Wiley InterScience (www.interscience.wiley.com).

ABSTRACT: The morphology and photoelectronic properties of blend films of poly(9,9′-dioctylfluorine) (PF) and ethyl–cyanoethyl cellulose [(E-CE)C] were investigated. It was found that the morphology of the blends was changed with the blend composition. The lateral phase separation was observed in submicron scale, and a nanoscale vertical phase separation occurred with enrichment of the (E-CE)C at the surface of the blend films. The photoluminescent spectra of the blend films are blue-shifted with the increase of the (E-CE)C. The photoelectronic properties of the blends varied with the morphology of the blends. In the electroluminescent device, the turn-on voltage was almost identical for the device with 50% or above 50 wt % PF in blend films and markedly improved for the device with only 25 wt % PF. The external quantum efficiency of the device fabricated with 75% PF is the highest among the device fabricated with the PF/(E-CE)C blend films. © 2007 Wiley Periodicals, Inc. J Appl Polym Sci 106: 1390–1397, 2007

Key words: polyfluorene; ethyl–cyanoethyl cellulose; blends; morphology; luminescence

INTRODUCTION

The blends of different conjugated polymers, as active emissive materials in light-emitting diodes (LEDs), have become increasingly important. This is because luminescent efficiency in resultant devices can be improved[1–4]; the colors can be easily tuned as the change of voltage[2–5] and white light can be obtained by the combination of polymers with blue, red, and green emission in the devices,[6–10] etc. When the conjugated polymer is blended with nonconjugated polymer, high efficient photoelectronic devices can also be obtained.[11–13] Furthermore, nanoscale light source was obtained due to nanodomains of conjugated polymers formed by phase-separation in blend films.[11]

In spite of significantly improving device performance by blend, a number of scientific challenges to more fully understand, quantify, and predict the properties of the blend LEDs according to the morphology of films remain. In fact, the morphology and structure of the blend film can be remarkably affected by the concentration of solution, the solvent, and the velocity of spin-cast besides thermodynamic factors, which in turn affects the optoelectronic properties of conjugated polymer blends. However, the studies on the phase behavior of the conjugated polymer blend films, especially on ultrathin films (less than 100 nm) that are directly used in LEDs, are scarce. The relationship between the phase behavior of blend films and the performance of the LEDs is far from to be clear.

Many nonconjugated polymers, such as poly(methylmethacrylate)(PMMA),[11,14,15] polystyrene,[13,16,17] and polyvinyl alcohol,[18] have been applied in conjugated polymer blends to improve the performance of the LEDs. Ethyl–cyanoethyl cellulose [(E-CE)C] is a semi-rigid molecule with its good properties for forming thin film, good transparency in the visible range, and large band gap. Hence, (E-CE)C can be used as a good candidate in nonconjugated/conjugated polymer blends.

In this work, the evolution of morphology of the polymer blends with blend composition was presented. The compositional dependence of the poly(9,9′-dioctylfluorine) (PF)/(E-CE)C blends on the photoluminescent (PL) and electroluminescent (EL) properties was studied. The effects of the morphology

Correspondence to: Y. Huang (yhuang@cashq.ac.cn).
Contract grant sponsor: National Natural Science Foundation of China; contract grant numbers: 50473057, 20374055, 50521302.
Contract grant sponsor: Chinese Academy of Sciences; contract grant number: KJCX2-SW-H07.

of the blend films on the optoelectronic properties were discussed.

EXPERIMENTAL

Materials

PF was synthesized by using Suzuki polycondensation.[19] The number–average molecular weight of PF was 1.5×10^4, determined by gel permeation chromatography calibrated with polystyrene standard. (E-CE)C was obtained by the reaction of ethyl cellulose with acrylonitrine.[20] The degree of substitution for ethyl was about 2.1 and for cyanoethyl was about 0.4, determined through elemental analysis (CHN-O-RAPID, Heraeus, Germany).

Preparation of solutions and LED devices

The individual polymer solution was prepared by dissolving the homopolymer in toluene at a concentration of 8.3 mg/mL and was stirred with a magnetic bar at 45°C for 12 h. The homopolymer solutions were filtered using 0.45 μm filter to remove undissolved particles. The polymer blend solutions were prepared by mixing the corresponding homopolymer solutions to obtain the required composition.

The active films used in LEDs were fabricated with spin-coating of the polymer blend solutions at room temperature. The rate of spin-coating was adjusted in the range of 1500–3000 rpm to obtain the active films with the almost identical thickness. The device structure is indium tin oxide (ITO) glass/poly(3,4-ethylene dioxythiophene) (PEDOT)/conjugated polymer film/Al film. The etched ITO glass was cleaned in ultrasonic bath with aqueous detergent, deionized water, acetone, and isopropanol, respectively. Then, it was dried at 120°C for 2 h. The thickness of the PEDOT film, conjugated polymer film, and Al film was 30 ± 5, 50 ± 5, and 100 nm, respectively.

Measurements

The sample films for atom force microscope (AFM) (NanoScope lllA Mutimode AFM, Digital Instruments) measure were obtained from the device films. The films for transmission electron microscope (TEM) (JEM-100CXΠ) measure were prepared by floating the films off PEDOT-coated glass substrates with deionized water onto Cu grids.

X-ray photoelectron spectroscopy (XPS) measure was carried out with a VG ESCA Lab 220i-XL X-ray electron spectrometer. Al Kα X-ray source (1486.6 eV) was used as the anode and operated at 15 kV and 18 mA. The pass energy of the analyzer was fixed at 40 eV. The binding energy (BE) scales for these samples were referenced by setting the alkyl C1s BE to 284.6 eV. The take-off angle used for analysis was 90° and 15°. The relative amounts of different bound carbons were determined from high-resolution C1s spectra and only C1 peak was fixed at 284.8 eV in the curve fitting process.

UV–vis absorption spectra were recorded with a UV–vis spectrophotometer (SHIMADZU, UV-1601PC) and steady state PL spectra were measured with a fluorescence photometer (VARIAN, Cary Eclipse, FLR025) at room temperature.

RESULTS AND DISCUSSION

The morphology of PF film and the blend films

The films of neat (E-CE)C and PF were examined firstly by AFM. It was found that there was no discrete morphological feature for neat (E-CE)C film. Although some ''short bars'' in neat PF film surface with the height difference being less than 5 nm can be observed in Figure 1(a–c), highly magnified phase image reveals that the ''short bars'' are 55–70 nm in length and 10–15 nm in width [Fig. 1(d)]. They should be lamellae of PF. The formation of lamellae of PF is possible due to residual solvent after high velocity spin-casting[21] and lower glass-transition temperature (T_g) of PF in the film surface compared with that of PF bulk,[22] which makes the motion of PF chains very easy.

Addition of 25% (E-CE)C into PF, i.e., 75% PF in the blend, leads to distinct higher-lying round particles surrounded by lower-lying matrix (Fig. 2). The particles range from 100 to 200 nm in diameter and 5–10 nm in height. From the phase image of higher magnification [Fig. 2(d)], the higher-lying domains have no fine structure. Although many ''short bars'' are also observed in lower-lying surface of the film, the size of which is consistent with that in neat PF film in Figure 1, the short bars in this film surface should be the lamellae of PF, too. It is speculated that lower-lying phase may be PF or PF-rich phase and the higher-lying particles may be (E-CE)C or (E-CE)C-rich.

Evidently, the phase separation occurs in the PF/(E-CE)C blend. The miscibility of two polymers depends on the mixing free energy, which in turn depends on both enthalpic (ΔH) and entropic (ΔS) contributions. In general, ΔH is positive, and ΔS is small for polymer blends. Compared with flexible polymer chains, the blends of rigid polymer and semirigid polymer result in a smaller ΔS, which results in that the phase separation is easier.

As to the formation of the morphology that the domains bloom on the film surface, it has been believed to be related to the solubility of individual polymer in solvent.[5,23] The polymer that dissolved

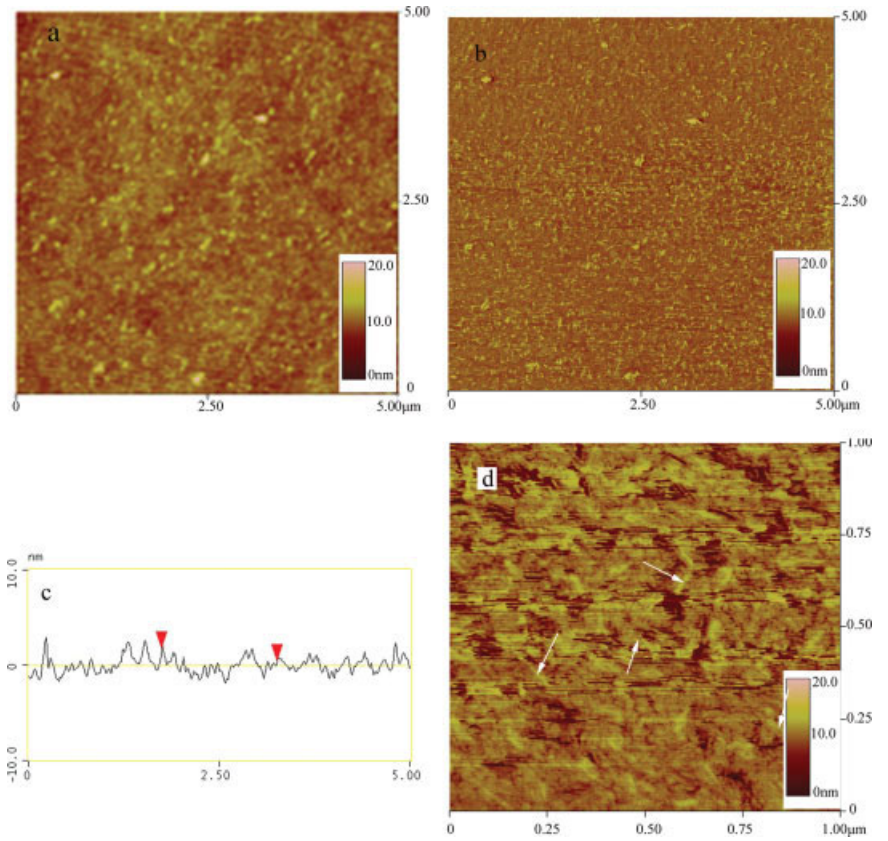

Figure 1 AFM images of neat PF film, (a) height image; (b) phase image; (c) section analysis; (d) the phase image with higher magnification. [Color figure can be viewed in the online issue, which is available at www.interscience.wiley.com.]

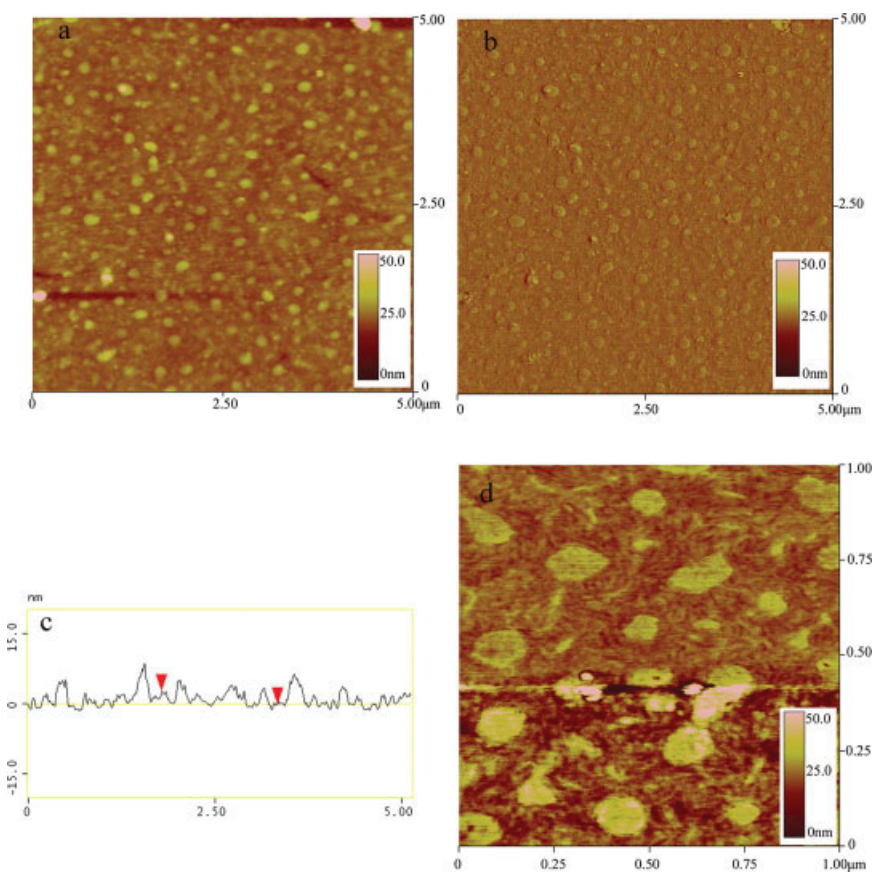

Figure 2 AFM images of 75% PF blending film, (a) height image; (b) phase image; (c) section analysis; (d) the phase image with higher magnification. [Color figure can be viewed in the online issue, which is available at www.interscience.wiley.com.]

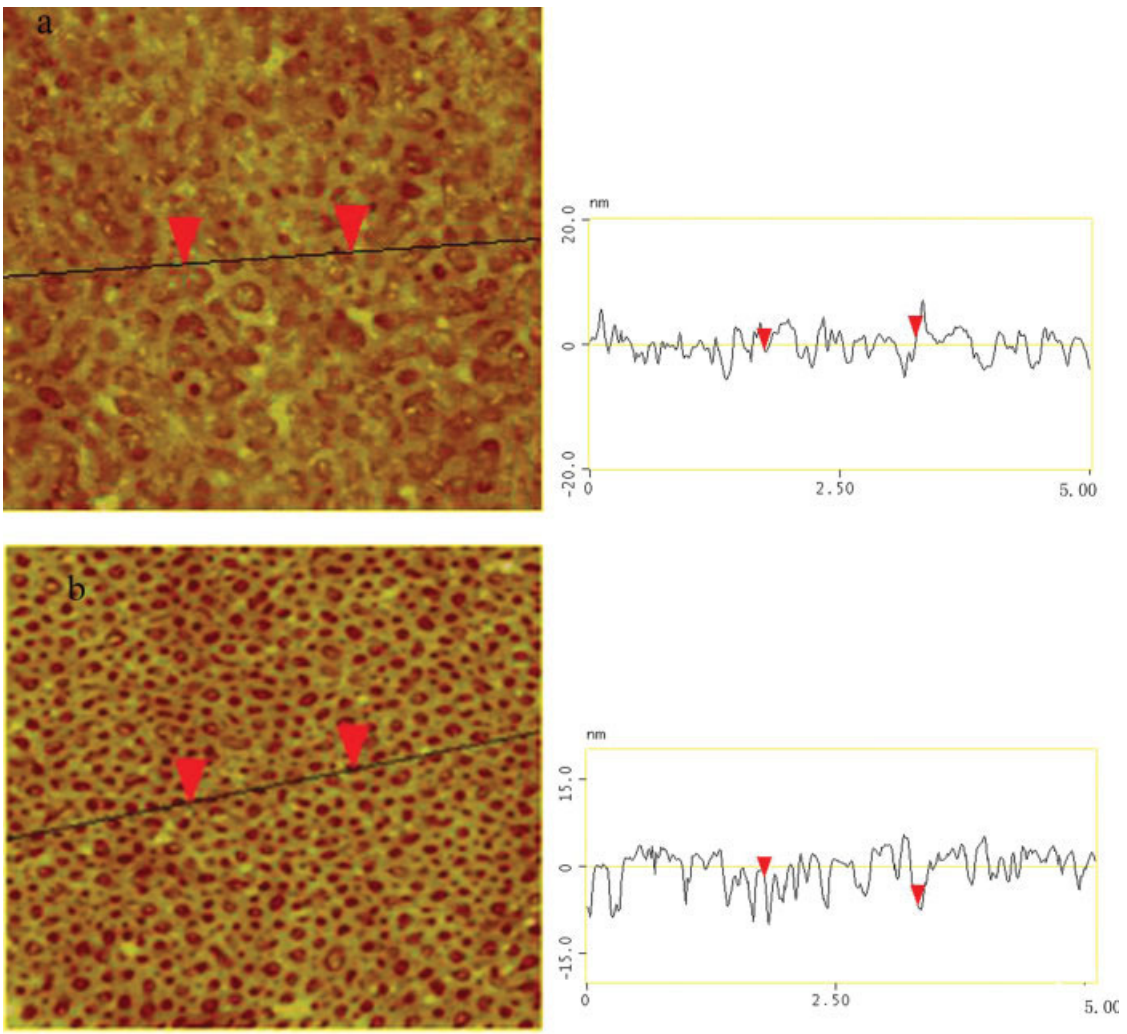

Figure 3 AFM high images (left) and section analysis (right) of 50% (a) and 25% (b) PF in the blends. The sizes of images are 5 × 5 μm^2. [Color figure can be viewed in the online issue, which is available at www.interscience.wiley.com.]

better in the solvent tends to depress to the surface of the blend film, and the polymer that dissolved poorer in the solvent tends to bloom to the surface of the blend film. The solubility of a given polymer in a solvent is mainly judged by the solubility parameters (δ) of the polymer and solvent. If the solubility parameter of the polymer is similar to that of solvent, the polymer can be dissolved in the solvent. The δ of toluene, PF, and (E-CE)C were calculated using group contribution methods with data tables of Van Krevelen.[24] The δ of toluene, PF, and (E-CE)C is 17.6 ± 1, 17.2 ± 1, 18.2 ± 1 $(J/cm^3)^{1/2}$, respectively. PF and toluene are all nonpolar molecules, whereas (E-CE)C is a polar molecule. From these results, it is predicted that toluene is a better solvent for PF than for (E-CE)C, which results in that (E-CE)C tends to bloom to the surface and PF is depressed to the surface.

Figure 3 shows the AFM results of the blends with 50 and 25% PF, respectively. For the blend of 50% PF, a bicontinuous network structure is observed in Figure 3(a). Both higher-lying phase and lower-lying phase exist in the height image. The higher-lying phase forms network structure; the ''network

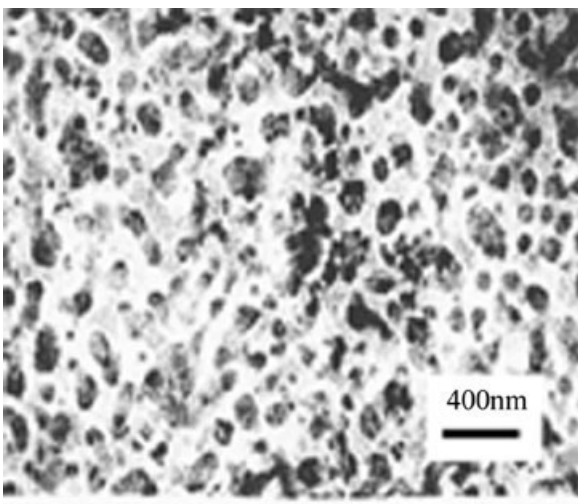

Figure 4 TEM image of 25% PF in the blend.

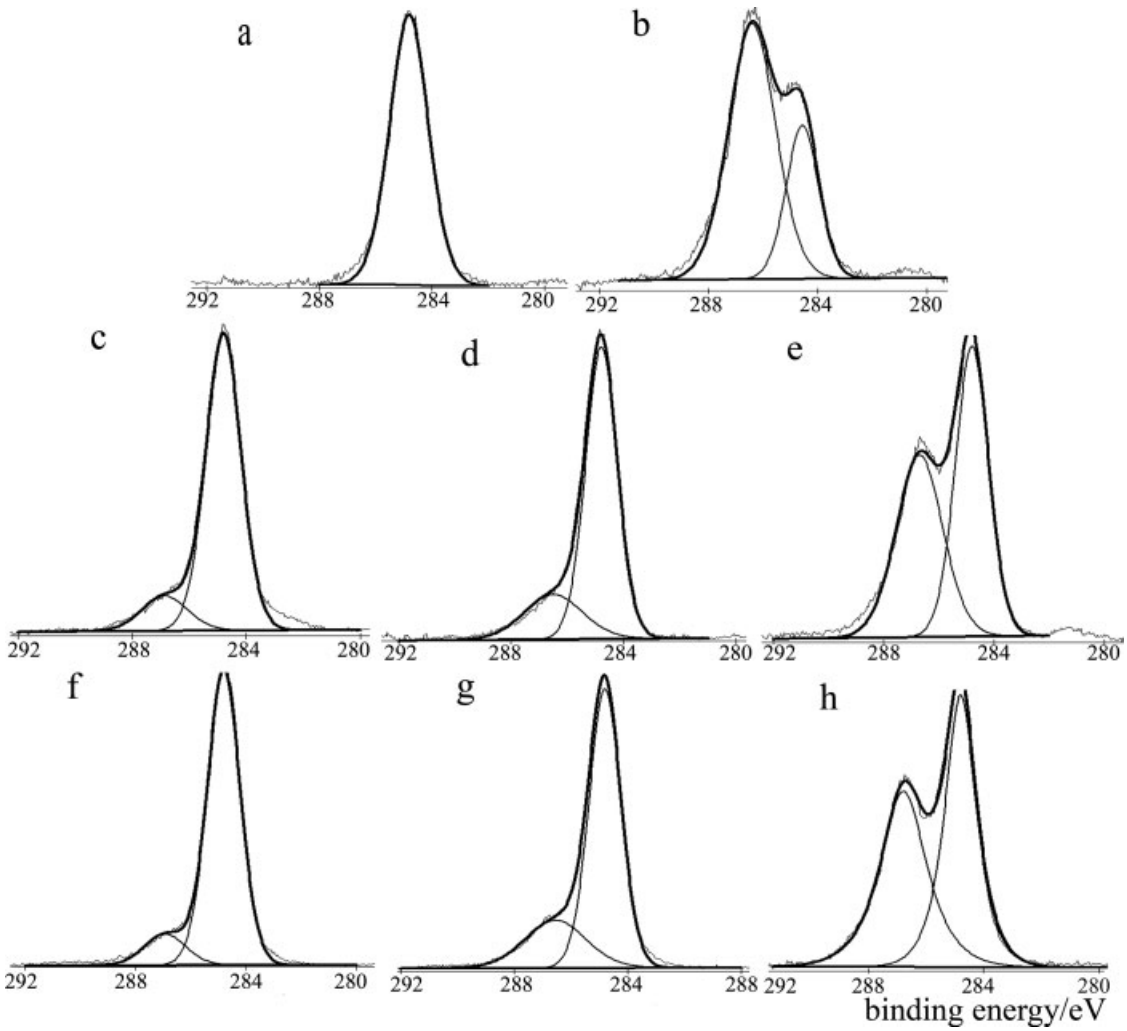

Figure 5 Deconvoluted XPS spectra of C1s for PF (a) and (E-CE)C (b) and their blends with 75% (c, f), 50% (d, g) and 25% PF in the blends, the takeoff angle for a–e spectra is 15° and for f–h spectra is 90°.

hollows'' are about 250–350 nm in diameter with a height difference of about 10 nm.

For the blend of 25% PF [Fig. 3(b)], the lower-lying phase is surrounded by the higher-lying phase to form hollow structure. The diameter of the hollows is about 100–200 nm with a depth of 5–8 nm. The depth is far less than the thickness of the film that is about 50 nm. That is, the higher-lying phase becomes the continuous phase and the lower-lying phase becomes the domains, which is further demonstrated by TEM.

TABLE I
The Data of Individual Polymer Films and Blending Films from XPS Spectra

PF in blend, theory (wt %)	Takeoff angle (degree)	PF, exp. (wt %)	(E-CE)C, exp. (wt %)	Relative enrichment of (E-CE)C (wt %)
100	15	100	0	–
75	15	63	37	48
	90	64	36	44
50	15	43	57	14
	90	45	55	10
25	15	19	81	8
	90	21	79	5.3
0	15	0	100	–

TEM image for the blend of 25% PF is shown in Figure 4. It can be found that the black clumps are surrounded by the white continuous phase. The black clumps are the conjugated polymer phase, and the white continuous phase is (E-CE)C. It is reasonable that the conjugated polymer has a stronger ability of scattering electrons than that of (E-CE)C because of the π-stacks of the conjugated polymer chains. Ananthakrishnan et al.[5] have also demonstrated that the black clumps are the conjugated polymers in poly[2-methoxyl-5-(2′-ethylhexyloxy)-1,4-phenylenevinylene] (MEH-PPV)/PF/PMMA blends by TEM. From the TEM image, (E-CE)C forms the continuous phase and PF forms domains in the blend film with 75% (E-CE)C, which is similar to

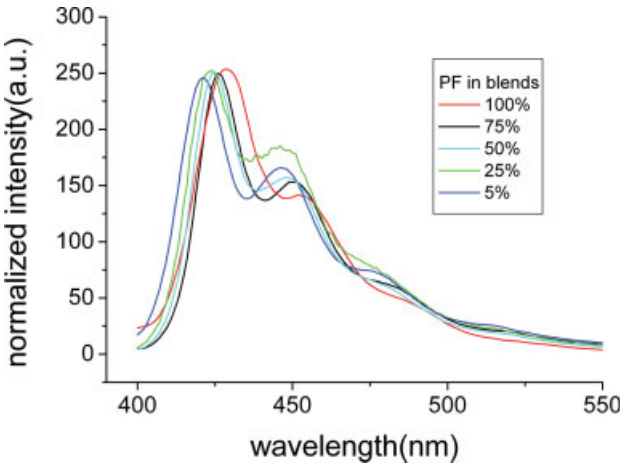

Figure 6 The PL spectra of blending films with different blending ratio. [Color figure can be viewed in the online issue, which is available at www.interscience.wiley.com.]

those observed by AFM. But the shape and size distribution of black clumps obtained by TEM are slightly different from those obtained by AFM. This is because the information obtained by TEM is the spatially averaged over the whole thickness of the polymer film.

The results of AFM and TEM observations unambiguously indicate the existence of the phase separation in the submicron range in the PF/(E-CE)C blend film. And it can be also primarily concluded from the AFM observation that the vertical phase separation of the spin-casting film may occur. To further demonstrate this point, XPS has been used to analyze the content of the two polymers on the surface.

Observation by XPS

XPS spectra (C1s) are obtained at an electron takeoff angle of 15° and 90°, as shown in Figure 5(a–e, f–h), respectively. There is only C1 in C1s of PF because of only existing carbon and hydrogen atoms in the PF molecule. The location of C1 is at 284.8 eV with a full width at half-maximum (fwhm) of 1.6 [Fig. 5(a)]. There should be three bonding types of carbon atom, that is, C1, C2, and C3 in C1s XPS spectrum for (E-CE)C. C1 is corresponding to the carbon atoms being bonded only to hydrogen or carbon (C—H and C—C bonds), C2 is the carbon atom singly bounded to a nonketonic oxygen atom (—C—O—), and C3 is the carbon bonded to two nonketonic oxygen atoms (O—C—O).[25] To simplify, the C1s peak of (E-CE)C is only divided into C1 peak and the mixed peak of C2,C3 (denoted as C23, which carbons are bonded to oxygen) as shown in Figure 5(b). The peak of C1 in (E-CE)C is at about 284.8 eV with a fwhm of 1.4, whereas the peak of C23 in (E-CE)C at about 486.5 eV has a big fwhm of 2.02. The integral ratio of C1 to C23 in XPS spectra of (E-CE)C is 1 : 2.6. That is, there are 3.17 C1 atoms in (E-CE)C molecule (according to the chemical formula $C_{11.4}O_5H_{19.6}N_{0.4}$ of (E-CE)C), which is more than the value (2.5) theoretically obtained according to the structure formula of (E-CE)C repeat unit. This is because of the existing hydrocarbon impurity, which is mainly a systematic error.[26,27]

The content of PF and (E-CE)C in film surface can be calculated according to the values of C1 and C23 in blend films. The calculating results are shown in Table I. It can be found that the content of (E-CE)C in the film surface is higher than the bulk value. And the (E-CE)C content obtained from a takeoff angle of 15° is slightly higher that obtained from a takeoff angle of 90°. It is suggested that the vertical phase separation occurs. It is also found that the relative enrichment of (E-CE)C, which is defined as $[(\text{E-CE})C_{(\text{experiment})} - (\text{E-CE})C_{(\text{theory})}]/(\text{E-CE})C_{(\text{theory})}$, is decreased with the decrease of PF in the blends.

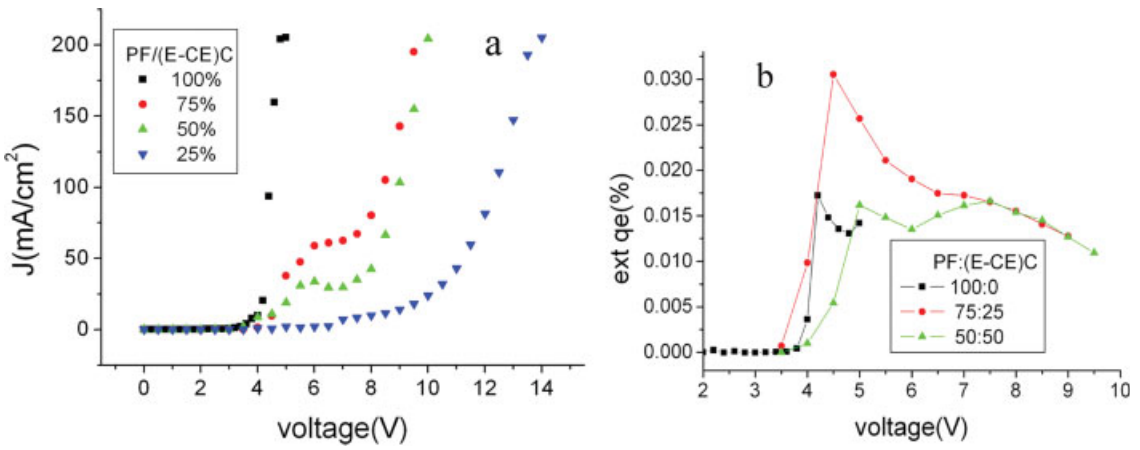

Figure 7 (a) current density–voltage curve for the devices with neat PF and PF/(E-CE)C blending films; (b) the external quantum efficiency (qe)–voltage curve for different content of PF. [Color figure can be viewed in the online issue, which is available at www.interscience.wiley.com.]

Toluene is a better solvent for PF relative to (E-CE)C. Thus, (E-CE)C will be separated out firstly and PF in toluene will expel (E-CE)C molecules to bloom to the surface with the evaporation of the solvent.[23] The expelling force decreases with the decreasing of the PF content in the blends, which may be related to the decrease of total surface energy. These results suggest the enrichment of (E-CE)C on the film surface, which is consistent with the results obtained by AFM observations.

PL and EL emissions of PF film and the blend films

Figure 6 shows PL emission spectra of the neat PF film and the PF/(E-CE)C blend films. It can be seen that the emission spectra of the films are blue-shifted with decreasing PF content. The neat PF have a main peak at 429 nm. When the PF content in the blend film is decreased to 5%, the main peak of PF is blue-shifted to 421 nm and is narrowed. The phenomena have also been observed in other blend systems.[14,18] It is suggested that PF chains are really separated by (E-CE)C molecules and the interaction of PF chains is decreased, which helps to improve the luminescent efficiency of the PF films.

The EL performance of the devices fabricated with the blends is investigated. The value of the LED properties was obtained by averaging three LED devices. The relationship between current density (J) and voltage (V) is shown in Figure 7(a). It is found that the turn-on voltage for the devices fabricated with 50% or above 50% PF in blends is almost identical,[13] about 3.6 V, and is increased to 9 V for the device with 25% PF. The phenomena could be related to the phase morphology of the blend film. From the AFM and TEM images, the PF is in continuous phase when PF contents are equal to or above 50% in the blend film, that is, the passage of the charges is continuous. And for the blend of 25% PF, the conjugated polymers are separated by (E-CE)C and formed domains, which may result in the increase of the resistance and then the increase of turn-on voltage of the device.[11]

The external quantum efficiency of PLED device was defined as N_P/N_E (N_P is the number of photos emitted externally from the device and N_E is the number of electrons injected in to it within unit time) and was calculated according to the literature.[28] The external quantum efficiency as a function of voltage for devices that contain different content of PF is compared as shown in Figure 7(b). Though the efficiencies for the devices are low, it is evident that the peak efficiency of the device with 75% PF is higher than that of the devices with neat PF and the other blend film. The variation of the efficiency of the devices can be because of the following reasons. As the (E-CE)C contents is increased, the PL spectra are blue-shifted and PL quantum efficiency is increased (mentioned above); furthermore, the efficiency of electron-hole capture will be increased at the heterojunctions of PF and (E-CE)C.[11,29] The above two factors can improve the EL efficiency. But (E-CE)C, as a insulator, can block the transport of electrons and holes, resulting in a lower combination efficiency of electrons and holes. Therefore, there exist in an optimal content of PF in the blend for the external quantum efficiency, which is about 75% PF in the blend.

CONCLUSIONS

The morphology of PF/(E-CE)C blend films varies with the composition of the blends. At a low (E-CE)C (or PF) content, (E-CE)C (or PF) can exist as an isolated domain and the other component as a continuous phase in the blends. A bicontinuous phase structure is observed when the composition of the blend is 50/50 of PF/(E-CE)C. (E-CE)C in the blends tends to bloom on the blend film surface. The PL spectra of the blend films are blue-shifted with increasing (E-CE)C composition in the blends. In the EL device, the turn-on voltage is almost identical for the devices with 50% or above 50% of PF in the active layer. And when PF is equal to 25%, the turn-on voltage is improved. It is also found that the efficiency of the device with 75% PF is the highest among the device fabricated with the PF/(E-CE)C blend films.

References

1. Yang, J.; Jiang, C. Y.; Zhang, Y.; Yang, R. Q.; Yang, W.; Hou, Q.; Cao, Y. Macromolecules 2004, 37, 1211.
2. Sainova, D.; Miteva, T.; Nothofer, H. G.; Scherf, U.; Glowacki, I.; Ulanski, J.; Fujikawa, H.; Neher, D. Appl Phys Lett 2000, 76, 1810.
3. Niu, Y. H.; Yang, W.; Cao, Y. Appl Phys Lett 2002, 81, 2884.
4. Corcoran, N.; Arias, A. C.; Kim, J. S.; MacKenzie, J. D.; Friend, R. H. Appl Phys Lett 2003, 82, 299.
5. Ananthakrishnan, N.; Padmanaban, G.; Ramakrishnan, S.; Reynolds, J. R. Macromolecules 2005, 38, 7660.
6. Yao, Y. H.; Kung, L. R.; Hsu, C. S. Jpn J Appl Phys Part 1 2005, 44, 7648.
7. Manoharan, S. S.; Mohammad, Q. Phys Status Solidi A 2005, 202, 1124.
8. List, E. J. W.; Leising, G.; Schulte, N.; Schluer, D. A.; Scherf, U.; Graupner, W. Jpn J Appl Phys Part 2 2000, 39, L760.
9. Heliotis, G.; Stavrinou, P. N.; Bradley, D. D. C.; Gu, E.; Griffin, C.; Jeon, C. W.; Dawson, M. D. Appl Phys Lett 2005, 87, 103505.
10. Chen, S. A.; Chang, E. C.; Chuang, K. R.; Chao, C. I.; Wei, P. K.; Fann, W. S. Abstr Pap Am Chem Soc 1998, 215, U392.
11. Iyengar, N. A.; Harrison, B.; Duran, R. S.; Schanze, K. S.; Reynolds, J. R. Macromolecules 2003, 36, 8978.
12. Tuladhar, S. M.; Poplavskyy, D.; Choulis, S. A.; Durrant, J. R.; Bradley, D. D. C.; Nelson, J. Adv Funct Mater 2005, 15, 1171.

13. He, G. F.; Liu, J.; Yang, Y.; Li, Y. F. Chin Sci Bull 2003, 48, 853.
14. Chou, H. L.; Hsu, S. Y.; Wei, P. K. Polymer 2005, 46, 49670.
15. Chappell, J.; Lidzey, D. G. J Microsc-Oxford 2003, 209, 188.
16. Harrison, B. S.; Foley, T. J.; Knefely, A. S.; Mwaura, J. K.; Cunningham, G. B.; Kang, T. S.; Bouguettaya, M.; Boncella, J. M.; Reynolds, J. R.; Schanze, K. S. Chem Mater 2004, 16, 2938.
17. Kang, T. S.; Harrison, B. S.; Foley, T. J.; Knefely, A. S.; Boncella, J. M.; Reynolds, J. R.; Schanze, K. S. Adv Mater 2003, 15, 1093.
18. Bjorklund, T. G.; Lim, S. H.; Bardeen, C. J. Synth Met 2004, 142, 195.
19. Miyaura, N.; Suzuki, A. Chem Rev 1995, 95, 2457.
20. Wang, L. G.; Huang, Y. Macromolecules 2002, 35, 3111.
21. Banach, M. J.; Friend, R. H.; Sirringhaus, H. Macromolecules 2004, 37, 6079.
22. Cossy-Favre, A.; Diaz, J.; Liu, Y.; Brown, H. R.; Samant, M. G.; Stohr, J.; Hanna, A. J.; Anders, S.; Russell, T. P. Macromolecules 1998, 31, 4957.
23. Kim, J. S.; Ho, P. K. H.; Murphy, C. E.; Friend, R. H. Macromolecules 2004, 37, 2861.
24. Van Krevelen, D. W. Properties of Polymers: Their Correlation with Chemical Structure; Their Numerical Estimation and Prediction from additive Group Contributions; Elsevier: Amsterdam, 1990.
25. Dorris, G. M.; Gray, D. G. Cellul Chem Technol 1978, 12, 721.
26. Gauthier, A.; Derenne, S.; Largeau, C.; Dupont, L.; Guillon, E.; Dumonceau, J.; Aplincourt, M. J Anal Appl Pyrolysis 2003, 67, 277.
27. Gauthier, A.; Derenne, S.; Dupont, L.; Guillon, E.; Largeau, C.; Dumonceau, J.; Aplincourt, M. Anal Bioanal Chem 2002, 373, 830.
28. Okamoto, S.; Tanaka, K.; Izumi, Y.; Adachi, H.; Yamaji, T.; Suzuki, T. Jpn J Appl Phys 2001, 40, L783.
29. Morteani, A. C.; Friend, R. H.; Silva, C. J Chem Phys 2005, 122, 244906.